MISSOURI S&T

Missouri University of Science and Technology

Scholars' Mine

Physics Faculty Research & Creative Works

Physics

01 Dec 1995

Upper-Tropospheric Aerosol Sampled During Project Fire IFO II

Donald E. Hagen
Missouri University of Science and Technology, hagen@mst.edu

Josef Podzimek
Missouri University of Science and Technology

Max B. Trueblood
Missouri University of Science and Technology, trueblud@mst.edu

Follow this and additional works at: https://scholarsmine.mst.edu/phys_facwork

Part of the Chemistry Commons, and the Physics Commons

Recommended Citation

D. E. Hagen et al., "Upper-Tropospheric Aerosol Sampled During Project Fire IFO II," *Journal of the Atmospheric Sciences*, vol. 52, no. 23, pp. 4196-4209, American Meteorological Society, Dec 1995.
The definitive version is available at https://doi.org/10.1175/1520-0469(1995)052<4196:UTASDP>2.0.CO;2

Upper-Tropospheric Aerosol Sampled during Project FIRE IFO II

DONALD E. HAGEN,* JOSEF PODZIMEK,[†] AND MAX B. TRUEBLOOD

Cloud and Aerosol Sciences Laboratory, University of Missouri at Rolla, Rolla, Missouri

ABSTRACT

During the FIRE IFO II project, aircraft were available for airborne sampling in and around cirrus clouds. Aerosols can play a role in the cloud formation process through the heterogeneous nucleation mechanism, and in turn, once formed, cirrus clouds can impact the ambient aerosol through scavenging and other collection mechanisms. University of Missouri aerosol sampling facilities were employed on these aircraft for in situ collection and characterization of the particulates near cirrus cloud level. Tandem differential mobility analyzer and impactor techniques were used to measure aerosol size distribution, hydration capability, and particle composition information. Evidence of aerosol layering was observed near the tropopause, and there was a tendency toward depletion of the ambient aerosol at both ends of the condensation nuclei (CN) size distribution. A large variability in the fine particle CN concentration was found, ranging from several tens to several thousands per cubic centimeter. The size distribution of particles larger than 0.5 μm roughly followed a lognormal relationship and large particle concentrations varied between 0.127 and 1.70 cm^{-3}. The particulates were found to be of mixed character, primarily inert with a small percentage of soluble material. A large variability in particulate concentrations was found.

1. Introduction

Research on cirrus cloud ice crystals has been quite active since pioneering work by Weickmann (1948). The microstructure of cirrus clouds and the morphology of ice crystals were the subject of many investigations by Heymsfield (e.g., 1972, 1973). He and his fellow workers paid attention to the generating processes of cirrus uncinus and their importance to precipitation development (e.g., Heymsfield 1975a,b, 1977) and, in general, to the parameterization of the size spectrum and shapes of high-altitude ice elements in terms of ambient temperature and water content (Heymsfield and Platt 1984). Since the time when investigators started to be very interested in the role high-altitude clouds might play in radiative energy transfer and its variability during the day and year in global and regional scales (e.g., Stephens 1980; Liou 1986; Stephens et al. 1990; Parungo 1995), several important questions surfaced: What is the major mechanism of cirrus cloud element formation? Can natural and manmade pollutants and contaminants, combined with large-scale airmass exchange affect the cirrus formation? How far can cirrus clouds alter the ambient aerosol's nature and physical properties, such as concentration, size distribution, and deliquescence?

The first question is related to the mechanism of drop freezing at high altitudes in the troposphere. Heymsfield and Sabin (1989) summarized their study with: "In recent measurements, liquid water was not detected in cirrus clouds below −40°C and, since there appear to be few ice-forming nuclei in the upper troposphere, ice nucleation evidently takes place by homogeneous freezing of solution droplets." This finding is supported by many observations and measurements by in situ sampling and by remote sensing (e.g., Heymsfield and Sabin 1989; Sassen et al. 1989; Sassen and Dodd 1989). Usually, ammonium sulfate cloud condensation nuclei (CCN) with masses between 10^{-16} g and 10^{-12} g (which corresponds to the dry radius range 0.024 μm < r < 0.51 μm) are taken to be the dominating CCN substance, which, combined with updraft velocity and parameters characterizing the state of the atmosphere, determines the homogeneous freezing of droplets.

However, it should be kept in mind that many of the ice crystals in cirrus clouds have lifetimes of several hours and that droplet freezing can be affected by different processes, such as heterogeneous and contact nucleation, freezing after the impaction of insoluble aerosol particles or supercooled cloud droplets. During the droplet–aerosol particle interaction the space and time

* Additional affiliation: Department of Physics, University of Missouri at Rolla, Rolla, Missouri.

[†] Additional affiliation: Department of Mechanical and Aerospace Engineering and Engineering Mechanics, University of Missouri at Rolla, Rolla, Missouri.

Corresponding author address: Dr. Donald E. Hagen, Cloud and Aerosol Sciences Laboratory, University of Missouri at Rolla, Rolla, MO 65401-0249.
E-mail: hagen@umrvmb.umr.edu

inhomogeneity of aerosol concentration and size distribution play an important role. The total concentrations of condensation nuclei (CN) and Aitken nuclei (AN) at the level of cirrus clouds vary between several hundred and a few thousand per cubic centimeter and are marked by considerable vertical inhomogeneity over the middle geographical latitudes (e.g., Podzimek 1990). This inhomogeneity of AN and CN concentrations is accompanied by an intensive variability in aerosol particle size distribution, as was clearly demonstrated in the case of AN by Podzimek et al. (1977). Condensation nuclei and AN refer to particles that will condense water when subjected to high supersaturations. Condensation nuclei concentrations are measured by exposing the particles to a high supersaturation of a fluid other than water, for example, butanol, to grow them to countable size, so their corresponding water supersaturation is not well defined. Aitken nuclei concentrations are usually measured in an expansion chamber by exposing the particles to a high water supersaturation just below the ion nucleation limit.

Anomalous large particle size distributions in the continental troposphere were documented by Blifford and Ringer (1969), and the peculiarities of particle size distribution close to the jet stream in relationship to tropopause folding were described, for example, by Cadle et al. (1969) and Yamato and Ono (1989). A very interesting cross jet stream transport by waves and potential new particle formation at high altitudes was described by Wilson et al. (1991). The very complex process of submicron and large particle transformation during the interaction with cloud elements at high altitudes is reflected in Hagen et al. (1994) and Podzimek et al. (1994).

This paper represents a continuation of the past effort of the investigators to depict the nuclei concentration variability and the peculiarities of ultrafine, fine, and large particle size distributions in and around cirrus clouds. The hydration properties (deliquescence) of aerosol particles were determined under the assumption that the soluble component of the nuclei was either ammonium sulfate or sulfuric acid. With reference to these major goals the article contains a section describing the experimental technique and data evaluation, the results of nuclei concentration measurements, ultrafine particle size distributions, and the estimated deliquescence of condensation nuclei. Finally, comparison of the obtained results with other investigations of similar or related phenomena will be made.

2. Experimental procedure and instrumentation

The main goals of the field observations and measurements performed during the First International Cloud Climatology Project Regional Project (FIRE) research project have been outlined elsewhere (e.g., Starr 1987). The flights of the Sabreliner research aircraft of the National Center for Atmospheric Research

(NCAR) were aimed to provide, besides the general meteorological parameters, the necessary information about cirrus evolution and transformation, cirrus cloud microstructure, and cloud element interaction with the environment. These data enable one to judge the influence of cirrus clouds on weather and climate evolution (e.g., Liou 1986). As was mentioned earlier, an important part of this complex program concerned the atmospheric aerosol and how its physical and chemical properties affect cirrus cloud formation.

The investigators from the Cloud and Aerosol Sciences Laboratory of the University of Missouri at Rolla (UMR) focused on the role of particulates. Aerosol measurements were made using the UMR Mobile Aerosol Sampling System (MASS) installed on the NCAR Sabreliner aircraft. The mission of this facility was to sample aerosols and determine a number of their physical and chemical properties; see Fig. 1. A tandem differential mobility analyzer scheme is employed (Rader and McMurry 1986). The differential mobility analyzers (DMAs) function as high-resolution size filters, passing only a quasi-monodisperse (in size) component of the sampled aerosol, and the size is selectable. A saturator is located between the two DMAs to grow the aerosol particles to their equilibrium sizes at nearly 100% relative humidity. The polydispersed sample air is passed through four times the length of saturator tubing needed to bring dry air to a relative humidity of 99.99% (Fitzgerald et al. 1980). The sheath air is passed through the prescribed length of saturator tubing to bring dry air to 99.99% relative humidity but it enters the saturator at nearly 100% relative humidity since it is continuously filtered and recycled. The saturator is integrated into the second DMAs housing and the combination is well insulated to keep the saturator
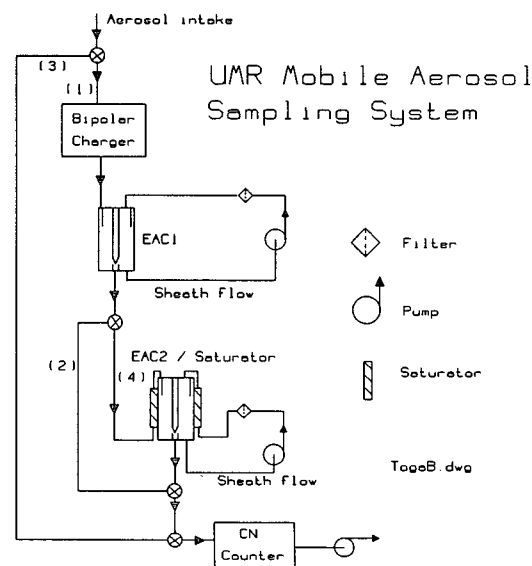

FIG. 1. UMR Mobile Aerosol Sampling System schematic.

and DMA2 at the same temperature. The tandem DMA can, in situ, acquire total aerosol concentration, size distribution, and hydration (critical supersaturation) information. In its Sabreliner configuration the support subsystems fit into two short 19-inch racks. The racks were separated by 15 inches to provide a space for the two DMAs, which were floor mounted. The air sample was drawn into the plane through a small tube, approximately ½-inch inner diameter, projecting through the aircraft skin; the exhaust line from the pumps is also projected out through the aircraft skin. For total CN concentration measurements an isokinetic sampling probe was used. During DMA size sweeps a non-isokinetic probe was used, but here we were operating in a size range that was not distorted by non-isokinetic sampling.

For total CN concentration measurements, outside air was directed along path 3 directly to a total particle counter. For this application the CN counter was a TSI (TSI Inc., St. Paul, Minnesota) butanol-type condensation nuclei counter (Model 3760). Particles larger than ~ 17 nm were counted. The CN counter efficiency correction factors developed by NCAR were employed.

In the size distribution measurement mode of operation, the sample air was directed along path 1 and given an electrical charge in the bipolar charger. The aerosol then passed through DMA1, and a selected size aerosol (monodispersed) emerged. Clean sheath air was provided by the pump and absolute filter. The monodispersed aerosol was directed around DMA2 via path 2 and on into the TSI CN counter. DMA1 was stepped through a series of voltages (aerosol particle sizes) and a particle concentration was taken at each particle size with the TSI CN counter. Hence, a size distribution was generated. Complicating factors, for example, the lower probability for putting an electrical charge on the smaller particles and the effects of multiple charges, were taken into account in the data inversion (Hagen and Alofs 1983).

In experiments to study the aerosol's hydration properties, outside air was size selected in DMA1 as above. The monodispersed aerosol passed via path 4 to the saturator integrated into DMA2. It was brought to nearly 100% relative humidity in the saturator, and the aerosol particles grew to their equilibrium size at this humidity. Information on the aerosol's hydration properties or critical supersaturation was contained in this equilibrium size. Even though the particles entering the saturator were monodispersed in size, a spectrum of particle sizes exited the saturator because of differences in particle chemistry and soluble mass fraction. The voltage on DMA1 was held fixed. The voltage (size setting) on DMA2 was then stepped through various values. The aerosol was passed onto the TSI CN counter, and a count was taken for each voltage setting of DMA2. These counts were then translated into a soluble mass fraction spectrum using Köhler theory and subsequently into a critical supersaturation spectrum

for the particles of the size given by DMA1. Then the size setting of DMA1 was changed, and the process repeated. Details of this procedure have been described elsewhere (Rader and McMurry 1986; Alofs et al. 1989; Hagen et al. 1992).

Laboratory experiments were undertaken to compare the aerosol critical supersaturation measurements given by the tandem DMA facility with those given by another device, the Continuous Flow thermal Diffusion cloud chamber (CFD). The CFD exposes the aerosol to a fixed supersaturation, and the value of the supersaturation is stepped through increasing values until a critical value of supersaturation is found that activates the aerosol as determined by an optical particle counter (Alofs 1978; Alofs et al. 1979; Alofs and Trueblood 1981). A laboratory burner (torch) was used to combust JP-5 jet fuel. The combustion aerosol was passed through a DMA to pick a specific particle size, and the critical supersaturation for this monodisperse aerosol was then measured by the CFD and deliquescence techniques. The results are shown in Fig. 2. The solid line shows the critical supersaturation spectrum for a laboratory-generated NaCl aerosol, which serves as a standard reference. The dotted line gives a straight-line fit to the critical supersaturation spectrum for the combustion aerosol as determined by the CFD. The circles give critical supersaturation values for three specific sizes as determined by the deliquescence method. The agreement between the deliquescence technique and the CFD method is quite good for the three measurements taken.

During several flights, the coarse (diameter 0.2–2.5 μm) aerosol particles were collected on sensitized gelatin covered glass plates in an inertial impactor (UN-ICO, Fall River, Massachusetts), which was installed on the University of North Dakota Citation research aircraft. The UNICO impactor was operated at a vol-
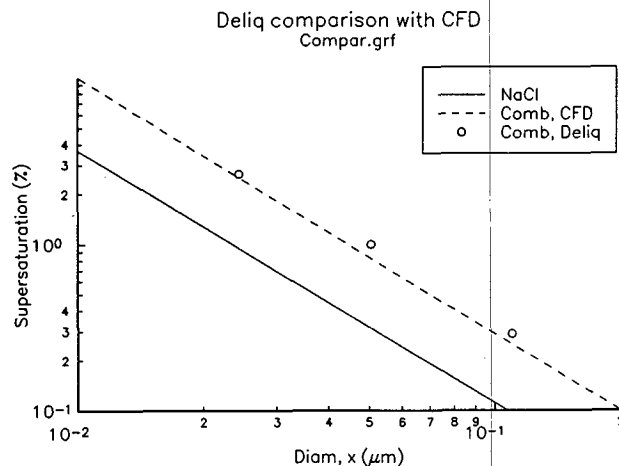

FIG. 2. Critical supersaturation spectra for combustion aerosols for comparison between the diffusion cloud chamber technique and deliquescence technique.

umetric airflow rate between 8 and 15 lpm. The details of the slide coating technique (BaCl₂ for sulfate ions and AgNO₃ for chloride ions) were described in our previous papers (Yue and Podzimek 1980; Hagen et al. 1994). Although evaluation difficulties were encountered (mainly in identifying sulfate ions), reasonably good information was obtained about the presence of supercooled droplets and the morphology of coarse insoluble aerosol particles in cirrus clouds (Podzimek et al. 1994). Approximately 1000 particles from each sample were identified. The impactor samples were examined also in a scanning electron microscope with an X-ray dispersive energy spectrum analyzer.

Most of the flights in and around cirrus clouds were performed over the central states (Kansas, Oklahoma, and Missouri) of the United States at the altitudes marked in the following figures and tables.

3. Concentration and size distribution of condensation nuclei

Results from the aerosol size distribution measurements with the UMR MASS are summarized in Table 1. Here h denotes the sampling altitude (km), T the temperature (°C), N the total particle concentration (number cm^{-3}), m the total aerosol mass (μg) in a 1200-liter air sample, assuming unit density, x the particle arithmetic mean diameter (μm) with standard deviation σ, x_s the particle mean surface diameter (μm), and x_v the particle mean volume diameter (μm). The total mass m is taken from the integral of the DMA-generated size distribution.

Looking at the total nuclei concentrations and their mean sizes, it is apparent that there is a great heterogeneity in the data, which is documented even during measurements at the same altitude (e.g., 26 Nov 1991). This is corroborated by the total CN concentration as measured directly by the TSI CN counter as shown in Fig. 3a. The gaps in the data correspond to times when total CN count was not being measured. The corresponding aircraft altitude profile is given in Fig. 3b. Turbulent heat and moisture fluxes govern cirrus cloud element formation and also the nucleation and aerosol particle scavenging by cloud elements. However, often at relative humidities higher than 75% with respect to water and favorable cryogenic absolute humidities indicating the possible presence of clouds, the corresponding ultrafine and fine particle concentrations were not minimal (e.g., the measurements on 5 and 6 Dec). It is not known in general which one of the mentioned sources of the aerosol concentration fluctuation, including the highly variable (in space and time) pollutants derived from aircraft engines, tend to be dominant. Furthermore, Table 1 shows clearly that at the same level (e.g., samples taken on 17 Nov at an altitude of 10.6 km within a time span of 12 minutes) the counts differ considerably compared to other samples (e.g., measurements on 26 Nov at an altitude of 10.0 km within approximately 12 minutes). Besides the measured minimum particle size, different sampling time, and aerosol concentration horizontal inhomogeneity, the aerosol stratification in the vertical direction plays an important role. Measurements on 5 and 6 December

TABLE 1. Average aerosol concentrations and size parameters.

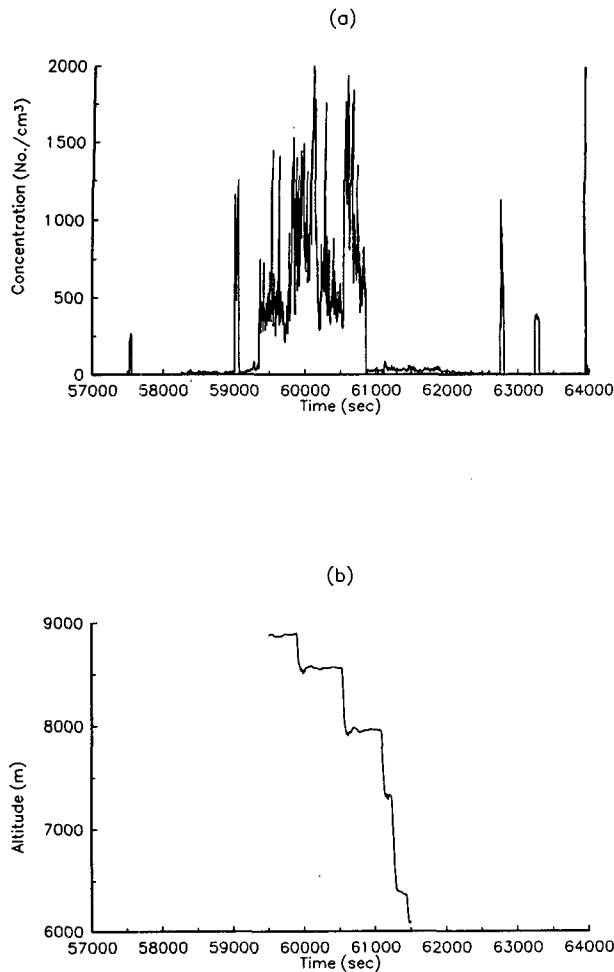| Date	Time	h (km)	T (°C)	N (cm^{-3})	m (μg)	x (μm)	σ	x_s (μm)	x_v (μm)
17 Nov 1991	1940	10.6	−49	113.23	0.003918	0.03365	0.01251	0.03590	0.03805
	1944	10.6	−48	2585.05	0.026592	0.02475	0.00348	0.02500	0.02539
	1947	10.6	−48	589.59	0.054692	0.03259	0.02478	0.04094	0.05285
	1951	10.6	−48	3736.03	0.037130	0.02460	0.00302	0.02479	0.02510
26 Nov 1991	1559	9.4	−51	1234.61	0.922022	0.08456	0.04562	0.09608	0.10590
	1603	9.4	−51	1244.47	0.765847	0.08093	0.04087	0.09067	0.09931
	1606	9.4	−51	16.33	0.009182	0.07046	0.04674	0.08455	0.09637
	1625	8.9	−46	1059.97	1.014438	0.09045	0.05159	1.04100	1.15100
	1656	7.4	−38	1207.72	0.725542	0.6863	0.04844	0.08400	0.09852
	1704	6.0	−22.7	1865.44	0.873794	0.06227	0.04425	0.07640	0.09067
	1727	10.0	−57	255.69	0.074825	0.05363	0.03842	0.06597	0.07752
	1731	10.0	−56	277.34	0.057945	0.04815	0.03391	0.05889	0.06928
	1735	10.0	−54	240.00	0.046774	0.04783	0.03212	0.05761	0.06769
	1739	10.0	−55	242.34	0.066023	0.05189	0.03769	0.06413	0.07569
	1743	10.0	−55	250.06	0.067714	0.05405	0.03613	0.06502	0.07554
5 Dec 1994	1538	5.6	−17	73.90	0.0272	0.07019	0.03168	0.07701	0.08370
	1726	11.9	−61	940.13	0.2010	0.05835	0.02506	0.06350	0.06981
	1729	11.9	−56	240.66	0.0785	0.07432	0.02127	0.07731	0.08039
	1742	9.4	−41.5	132.89	0.0397	0.06619	0.02903	0.07228	0.07807
6 Dec 1991	1459	6.1	−17	645.73	0.3650	0.07260	0.04183	0.08378	0.09654
	1502	7.5	−26	1058.80	1.9967	0.09091	0.07217	0.11610	0.14420
	1505	8.1	−31	599.36	0.7946	0.08829	0.06142	0.10750	0.12830
	1508	8.7	−35	336.88	0.1689	0.07351	0.03994	0.08366	0.09275

FIG. 3. Total CN concentration as function of time for flight on 26 Nov 1991 (a), with corresponding altitude profile (b).

particle transport from different sources on the ground and in the air and by the particle transformation due to interactions with other particles and cloud elements in the turbulent atmosphere. However, an attempt to single out the most important factors affecting standard deviation from the particle mean size did not lead to a simple conclusion. Humidity, possibly indicating a particle interaction with cloud elements, seems to be an important parameter. For relative humidities larger than 75% the mean standard deviation $\bar{\sigma}$ divided by the mean particle size $\bar{x}$ was 64.34% ($\pm 8.61\%$) calculated from nine independent measurements. The same parameter, calculated for samplings at relative humidities (RH) $\leq$ 75%, was 28.86% with a large standard deviation, $\pm 23.72\%$. Another potential parameter considered for contributing to the large variability of particle mean size was particle concentration. However, there was no clear correlation between these parameters. Nevertheless, the plotting of these data indicated that the smallest values of the parameter $\sigma/\bar{x}$ correspond often to very low concentrations of large hygroscopic particles as well as very large concentrations of small freshly generated particles probably related to aircraft emissions.

The particle (nuclei) size distribution was measured during seven flights on 17 and 26 November and 5–7 December 1991, which are described in Tables 5–8. Figure 4 demonstrates the differences of size distribution curves of nuclei sampled at the same level (10.6 km) during 12 minutes on 17 November. Common to all curves is the maximum differential concentration, dN/dx (plotted in number cm^{-4}), at about particle diameter 0.0235 μm and the minimum for particles larger than 0.07 μm. A secondary minimum in the particle size distribution was found to be around particle diameter 0.034 μm. The detailed comparison of all four curves is hampered by the fact that three curves were plotted with only four concentration points.

The 26 November samples displayed in Fig. 5 show some similarity but also some deviations when compared to the situation on 17 November. The average particle concentration (diameters between 0.017 and 0.024 μm) is apparently lower than in Fig. 4. However, in lower altitudes (between 6.0 and 9.4 km) the curves indicate the higher counts of particles with diameters larger than 0.07 μm, and in general, the effect of aerosol transport from lower levels of the troposphere is apparent in particle sizes larger than 0.03 μm. The sim-

document clearly this stratification. A dramatic change happened between 6.0 and 11.9 km, and the mean particle concentration (measured by the UMR MASS) did not follow the ideal decreasing trend of CN counts with increasing altitude [see the survey in Pruppacher and Klett (1978) or Podzimek (1990)]. Corresponding to the above-described particle concentration changes in the horizontal and vertical directions were similar changes in total particle mass and all size parameters (x, x_s, x_v). The standard deviation σ of the measured diameters x is explained by the complex process of the

TABLE 2. Flight 13 on 5 Dec 1991.

Run	Time (UTC)	Altitude [h(m)]	$\bar{x}$ (μm)	$\Sigma N(x)$ (cm^{-3})	x_0 (μm)	σ	N_0 (cm^{-3})
a	1538	6080	0.0702	73.9	0.0631	1.769	77.8
b	1727	11900	0.0584	940.1	0.0618	1.450	765.5
c	1729	11250	0.0743	240.7	0.0784	1.450	210.8
d	1742	9400	0.0662	132.9	0.0639	1.632	138.7

TABLE 3. Flight 15 on 6 Dec 1991.

Run	Time (UTC)	Altitude [(h(m)]	$\bar{x}$ (μm)	$\Sigma N(x)$ (cm^{-3})	x_0 (μm)	σ	N_0 (cm^{-3})
a	1500	6100	0.0726	645.7	0.0726	1.707	565.1
b	1502	7000	0.0909	1059.0	0.0844	1.932	670.9
c	1505	7900	0.0883	599.4	0.0811	1.911	571.7
d	1509	8600	0.0735	336.9	0.0644	1.873	310.2

ilarity of size distribution curves and the secondary minimum at 0.024 μm from the sampling at 10-km altitude is spectacular.

Different shaped size distributions appeared from the samplings at altitudes between 5.6 and 11.9 km on 5 December 1991 (Fig. 6). The two highest altitude samples taken at 1726 ($\square$) and 1729 ($\triangle$) UTC exhibit minima in dN/dx at small and large particle sizes and a distinct maximum around 0.038 μm (for the 11.9-km sampling, $\square$) and around 0.069 μm (for the 11.2-km sampling, $\triangle$), which might suggest that the sample contained a major stratospheric fraction of small particles. The slope of the large particle section of the size distribution curve for the 9.4-km altitude ($\triangledown$) is smaller than in Fig. 5. At this time there is no definite explanation for the surprising higher concentrations of the particles in the size range between 0.024 and 0.2 μm at altitudes above 11.0 km in comparison to lower-level concentrations.

Another example of particle size distributions in the nucleation–accumulation transition region is presented in Fig. 7. It contains four curves from the sampling on 6 December 1991 at altitudes between 6.1 and 8.7 km and corresponding temperatures from -17.5°C to -35.0°C. The curves have flat maxima between 0.04

and 0.08 μm and minima at smallest and largest particle sizes (0.018 and 0.303 μm). The highest nuclei concentration was measured at the altitude of 7.5 km, which was marked by a considerable increase of large particle concentration (8.406×10^6 cm^{-4} for $x = 0.303$ μm). No significant secondary minimum or high concentration of particles smaller than 0.02 μm in diameter was found.

Though the curves in Figs. 6 and 7 do not indicate a direct application of the lognormal fit, an attempt was made to apply the formula

$$\left(\frac{dN}{dx}\right)dx = \frac{N_0}{\sqrt{2\pi}(\ln\sigma)}\, e^{-(\ln x - \ln x_0)^2/(2\ln^2\sigma)} d\ln x \quad (1)$$

to the discrete data. Tables 2 and 3 summarize the results of calculations corresponding to Figs. 6 and 7. Here $\bar{x}$ denotes the aerosol's average diameter estimated from the discrete data, and $\Sigma N(x)$ the integrated total particle concentration estimated from the discrete data. The corresponding parameters, x_0 and N_0, were taken from the best lognormal fit. These two series of aerosol samplings at the cirrus cloud level document cases where the lognormal function gives a fairly good fit to the measured aerosol size distributions.

TABLE 4. Aerosol soluble mass fraction.

Date	Time (UTC)	Altitude [h(m)]	x (μm)	R((NH$_4$)$_2$SO$_4$)	R(H$_2$SO$_4$)
5 Dec 1991	1544	8300	0.060	0.100	0.072
	1604	9100	0.088	0.041	0.030
	2028	8850	0.062	0.220	0.160
6 Dec 1991	1526	9500	0.089	0.020	0.014
	1532	9500	0.089	0.018	0.013
	1927	7200	0.081	0.041	0.029
	1932	8300	0.088	0.038	0.028
	1938	9000	0.086	0.034	0.024
	1942	8200	0.084	0.059	0.043
	1944	8200	0.056	0.240	0.170
7 Dec 1991	2010	8500	0.042	0.100	0.058
	2013	8200	0.042	0.100	0.058
	2017	7800	0.041	0.069	0.038
	2019	7400	0.040	0.082	0.044
	2033	7300	0.117	0.100	0.078
	2057	7300	0.121	0.050	0.038
	2100	7300	0.124	0.050	0.039
	2103	7800	0.126	0.041	0.032
	2107	8900	0.129	0.057	0.044
	2110	9350	0.131	0.021	0.016

TABLE 5. Positions where aerosol size distributions were measured for the 17 Nov 1991 flight.

Run	Time (UTC)	Altitude (km)	Long (deg)	Lat (deg)
a	1941	10.6	95.644	37.789
b	1944	10.6	95.497	37.597
c	1947	10.6	95.572	37.391
d	1951	10.6	95.176	37.183

TABLE 7. Positions where aerosol size distributions were measured for the 5 Dec 1991 flight.

Run	Time (UTC)	Altitude (km)	Long (deg)	Lat (deg)
a	1538	5.6	95.759	36.95
b	1726	11.9	96.637	36.622
c	1729	11.2	96.935	36.639
d	1732	9.4	96.585	36.82

4. Deliquescence of condensation nuclei

The hydration properties, or deliquescence, of particles are characterized by the ratio of soluble mass to the total dry mass of the particle. This soluble mass fraction ratio, R, is calculated from the results of the described measurements under the assumption that the chemical nature of the soluble material is known. Table 4 summarizes the results of the calculations, which are based on Köhler's theory (e.g., Pruppacher and Klett 1978) for the case that all the soluble material is ammonium sulfate or sulfuric acid. The corresponding mass ratios are denoted by $R((NH_4)_2SO_4)$ and $R(H_2SO_4)$.

From the 20 aerosol deliquescence measurements at different altitudes one cannot make conclusions of general statistical validity. However, the deduced mean mass ratio of ammonium sulfate $R((NH_4)_2SO_4)$ can be used for the comparison with other investigations of this kind (e.g., Yamato and Ono 1989). The data in Table 4 also enables one to study the dependence of the mean values of $\bar{x}(\mu m)$, $\bar{R}(H_2SO_4)$, and $\bar{R}((NH_4)_2SO_4)$ on altitude. For measurements made between 7.0 and 8.0 km these values are $\bar{x}(\mu m)$ = 0.0929 μm, $\bar{R}(H_2SO_4)$ = 0.0426, and $\bar{R}((NH_4)_2SO_4)$ = 0.0619. Between 8.0 and 9.0 km these values are 0.0704 μm, 0.0791 μm, and 0.1143 μm, and between 9.0 and 10.0 km they are 0.0966 μm, 0.0194 μm, and 0.0268 μm, respectively. Tentatively, one could conclude that between 8.0 and 9.0 km smaller particles are prevailing, however, with a larger

content of soluble material, possibly injected by aircraft engines. Recent ground-based jet engine exhaust measurements (Frenzel and Arnold 1994) have indicated the presence of substantial amounts of gas phase HNO_3 and H_2SO_4, which may promote significant gas to particle conversion in a young exhaust plume. Surprising is the fact that larger particles with small contents of soluble material are found at higher levels of the troposphere. This interesting conclusion requires a systematic investigation in the future and comparison with a detailed analysis of the meteorological and aerological situation that affects the exchange of aerosol particles.

5. Sampling of large and coarse particles

Samplings of particles larger than 0.25 μm were performed with a four-stage inertial impactor (UNICO) on slides coated for qualitative determination of the presence of chloride or sulfate ions in the aerosol particles. This technique and its calibration are described elsewhere (Yue and Podzimek 1980). It requires time consuming evaluation in optical and electron microscopes.

The use of the UNICO impactor was preferred for its simple operation onboard the University of North Dakota Citation aircraft in spite of some problems related to the determination of the sampling efficiency and instrument calibration. Large errors (up to ±20%) are expected in detecting the concentration of particles with radii $r \leqslant 0.50$ μm. In spite of the application of the recommended correction by the impactor's manufacturer (Unico Technical Bulletin No 4865, Union Industrial Equipment Corp., Fall River, Massachusetts), the unknown particle mass and particle deposition in a corner flow—with a specific bouncing problem (Pod-

TABLE 6. Positions where aerosol size distributions were measured for the 26 Nov 1991 flight.

Run	Time (UTC)	Altitude (km)	Long (deg)	Lat (deg)
a	1559	9.4	95.105	38.004
b	1603	9.4	96.573	37.919
d	1625	8.9	96.898	37.908
e	1656	7.4	96.727	38.045
f	1704	6	96.854	37.976
g	1727	10	97.413	38.137
h	1731	10	97.926	38.255
i	1735	10	98.394	38.296
j	1739	10	97.979	38.013
k	1743	10	97.506	37.756

TABLE 8. Positions where aerosol size distributions were measured for the 6 Dec 1991 flight (Fig. 7).

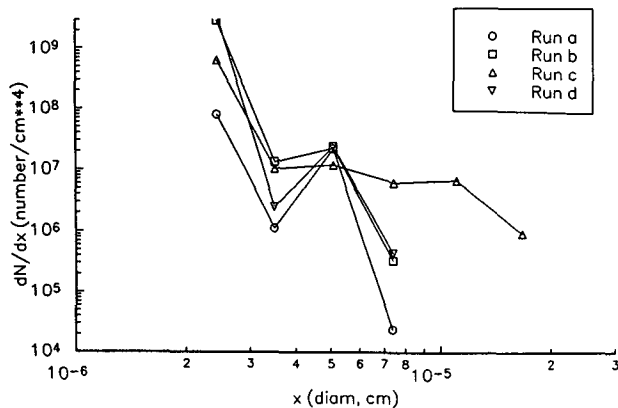| Run	Time (UTC)	Altitude (km)	Long (deg)	Lat (deg)
a	1459	6.1	95.474	37.099
b	1502	7.5	95.474	37.052
c	1505	8.1	95.745	36.942
d	1508	8.7	95.948	37.035

FIG. 4. Differential aerosol concentrations for samples taken during the 17 Nov 1991 flight. Sampling conditions given in Table 5.

zimek et al. 1991) — indicate that the concentrations of particles with radii greater than 2 μm shown in Fig. 8 have a relatively large uncertainty, about ±50% even with the total number of collected particles around 1000. During one sampling (1622 UTC 30 Nov 1991), the impactor volumetric flow rate was below 8 lpm, which affected strongly the impactor's particle collection efficiency, determined by use of the efficiency diagram supplied by the manufacturer. The diffusional and inertial losses of particles of the considered size in the inlet tubing (1.22 m long and 8 mm I.D.) from the probe to the impactor, which was placed in a cylindrical container 12.5 cm long and 6.6 cm I.D., were neglected.

The correction for isokinetic sampling at the airspeed between 3.5 and 5.5 m s^{-1} at the tube inlet and for an aircraft speed of approximately 180 m s^{-1} was considered because it affects the ratio of observed (measured by the impactor) to the true large particle concentrations. This ratio was calculated according to the formula by Badzioch (1960)

$$\frac{N_s}{N_0} = 1 - \alpha + \alpha\left(\frac{V_0}{V_s}\right), \qquad (2)$$

where N_s and V_s denote concentration and air sampling speed for a specific size particle, N_0 is the particle's concentration in the environment, and V_0 is the aircraft speed. The parameter α is related to the distance, L, ahead of the sampling tube where the particles (of a specific size) start to deviate from a straight line trajectory parallel with the axis of the sampling probe and to the particle stop distance, $l_p = 2V_0 r_p^2 \rho_p/(9 \mu)$. The particle stop distance was calculated for differently sized particles under the assumption that $V_0 = 180$ m/s, $\rho_p = 2.0 \times 10^3$ kg m^{-3} and that the air dynamic viscosity at the altitude 8 km was $\mu = 1.503 \times 10^{-5}$ kg m^{-1}s^{-1}. Using Badzioch's approach, L was found to be close to 4.0 cm. This value was used in the for-

mula for α, which, according to Badzioch (1960), has the form

$$\alpha = [1 - \exp(-L/l_p)]/(L/l_p). \qquad (3)$$

The Badzioch approach was selected for its simplicity and reasonably good results (e.g., Podzimek et al. 1984) and applied while calculating the data in Fig. 8 from the flights described in Table 9. Note that other correction formulations have been developed for non-isokinetic sampling (Davies 1968; Watson 1954).

The corrected size distribution curves in Fig. 8 show some similarity with the results of field aerosol measurements performed in 1990 and published elsewhere (Podzimek et al. 1994). There are deviations from the ideal Junge distribution, even if one disregards the distorted concentrations of particles with the radius $r = 0.25$ μm and of particles larger than $r = 2.00$ μm as discussed above. In the latter case the statistical errors, due to the small numbers of counted particles with $r > 2.00$ μm, can surpass ±50% of the calculated mean concentration.

The chemical composition of some typical large and coarse aerosol particles was determined qualitatively by evaluating the X-ray dispersive energy spectrum diagrams of typical particles found in the gelatinous layer that coated the slides. After subtracting the background in the diffracted X-ray spectrum due to the presence of gelatin components and the glass substrate, typical particle elements were determined. The background was represented in essence by Si and Ca ions in the ratio of approximately 1.00:0.24. Chloride ions represent usually a minor component of the background (Si/Cl is equal to 1.00:0.10). Besides these elements the analysis of 31 typical particles (in reference to their size and their shape) demonstrated the presence of the following elements arranged according to their mean relative concentrations (referred to Si background): C(44.8%), S(30.1%), Al(14.4%), Na(12.0%), Mg(11.8%), P(10.2%), K(7.5%), Fe(2.8%), and Ba(1.1%). Due to the arbitrarily chosen particles this is a very rough approximation to the real situation; however, these elements correspond roughly to those found in coarse particles during an aircraft aerosol sampling in 1990 (Podzimek et al. 1994).

6. Discussion

The results of the aerosol investigation at cirrus cloud level will be discussed in reference to the total CN and coarse particle concentration, then to the size distribution of CN and coarse particles, and finally, the interpretation of the nuclei deliquescence measurement will be presented.

In general, the difficult comparison of CN measurements persists since the time when Cadle and Kiang (1977) tried to compare the first systematic measurements made by Junge et al. (1961) at higher altitudes with their successors. It was clearly demonstrated that
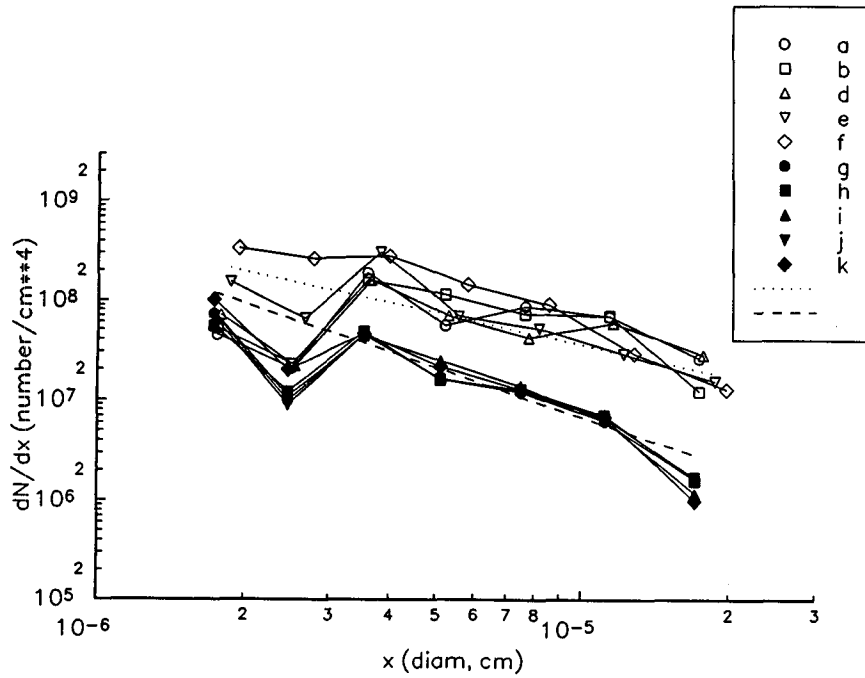
FIG. 5. Differential aerosol concentrations for samples taken during the 26 Nov 1991 flight. Sampling conditions given in Table 6. Dotted line: the trend in the lower-altitude data and dashed line: the trend in the higher-altitude data.

the use of different supersaturations of different condensing materials in the various counters, different particle losses in the sampling systems, and the large variability of nuclei concentrations in space and time caused serious problems, especially if the measurements were performed close to the tropopause and to air traffic corridors.

The above CN measurements do not deviate much from those of other authors in the following points: 1) The average concentrations measured at altitudes be-
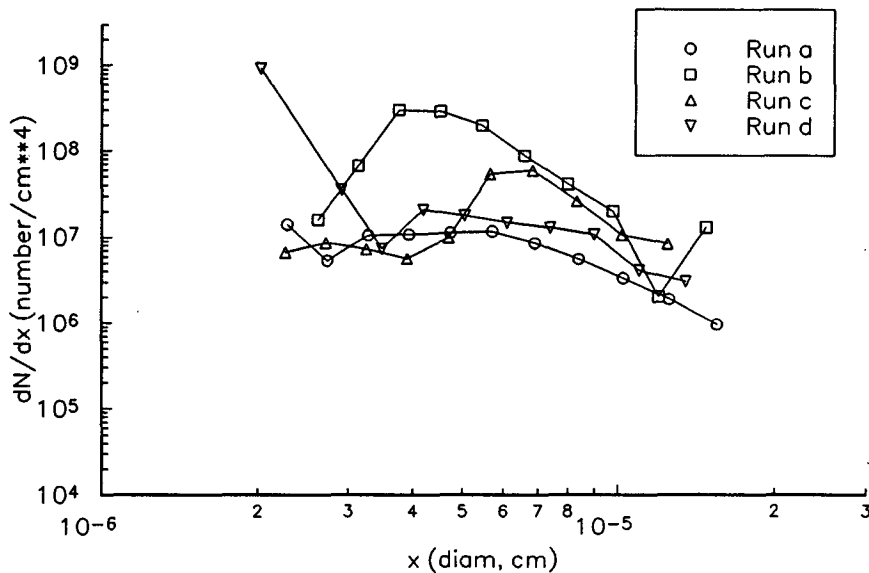

FIG. 6. Differential aerosol concentrations for samples taken during the 5 Dec 1991 flight. Sampling conditions given in Table 7.
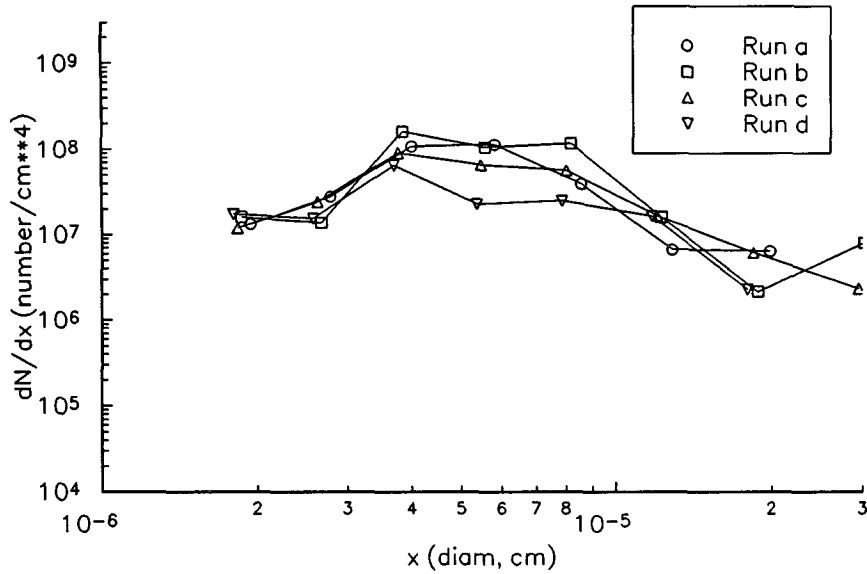
FIG. 7. Differential aerosol concentrations for samples taken during
the 6 Dec 1991 flight. Sampling conditions given in Table 8.

tween 6 and 12 km are comparable with other reported values (e.g., see Cadle and Kiang 1977). 2) The considerable variability of CN concentrations in the vertical and horizontal directions, especially in relationship to air traffic, was reported by Briehl (1974) and by Podzimek et al. (1977). 3) Inside of cirrus clouds CN concentrations were usually found to be small. Some of the large CN fluctuations and layer type dis-

tributions observed above and within cirrus clouds can be related to the proximity to the jet stream (e.g., 5 and 6 Dec) and to potential aerosol transport from its anticyclonic region to the jet's cyclonic side often accompanied by large-scale oscillations (Wilson et al. 1991). In addition, the large aerosol concentration and size variability and cirrus cloud alterations were identified by ground-based and airborne measurements over the
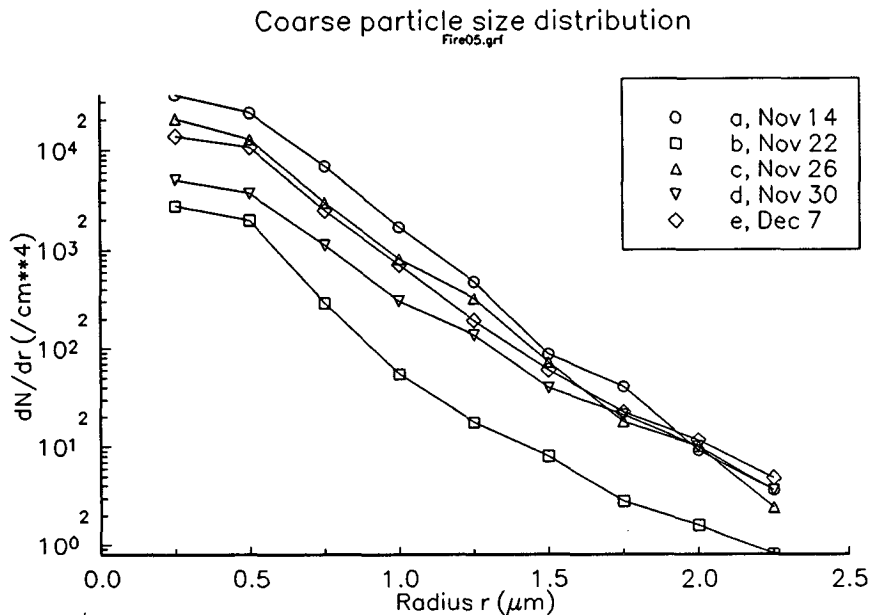

FIG. 8. Differential size distribution for large and coarse particles sampled with the UNICO
impactor on the University of North Dakota Citation. Sampling conditions given in Table 9.

TABLE 9. As in Table 8 (Fig. 8).

Run	Date	Time (UTC)	Altitude (km)	Long (deg)	Lat (deg)
a	14 Nov 1991	1603	7.8	95.39	37.228
b	22 Nov 1991	1938	7.2	94.818	37.693
c	26 Nov 1991	1727	9	95.538	37.11
d	30 Nov 1991	1622	10.9	95.2	36.488
e	07 Dec 1991	2107	9.2	92.837	33.42

central parts of the United States on 4–6 December (Sassen et al. 1994). The abnormally high ice crystal concentrations in cirrus clouds were related to the volcanic aerosols released during the June 1991 Mount Pinatubo eruptions and transported into the stratosphere around the globe. The interaction of southwesterly and northwesterly jet streams, which on 5 December extended to the Kansas–Oklahoma border, could be responsible for intense stratospheric–tropospheric exchanges of aerosol particles and ice crystal formation. This can explain the broad aerosol size distributions on 5 and 6 December (Figs. 6 and 7) and, possibly, the higher coarse particle concentrations on 7 December (Fig. 8). Another interesting conclusion can be taken from the aerosol deliquescence measurements. The two highest soluble mass fraction ratios (2028 5 Dec and 1944 6 Dec) were measured just below the base of cirrus clouds. Analysis of the sampling plane's flight trajectory and the observed wind velocities indicates that during the 1944 6 December sampling the plane may have flown through its own exhaust plume, but this was certainly not the case with the 2028 5 December sampling. Intense exchange of stratospheric and tropospheric aerosol is possibly responsible for the unusually high concentrations measured on 5 December at an altitude of 11.8 km and on 6 December at 7.5 km. This effect, combined with tropopause folding (e.g., Cadle et al. 1969; Yamato and Ono 1989), can probably also explain the considerable CN concentration variability in the four samples taken at 3-minute intervals at an altitude of 10.6 km on 17 November 1991.

Nuclei size distribution curves were already discussed in a previous section on CN sampling, which also includes the remark on the limited applicability of the lognormal size distribution formula to the measured counts. The 17 November 1991 sampling at an altitude of 10.6 km (Fig. 4) bears a resemblance to the curves typical for a tropospheric aerosol penetrating into the aerosol population in the lower stratosphere (e.g., Podzimek et al. 1977). Some indication for "saddle" type curves can be found in Fig. 5, where, however, the secondary minimum is shifted toward smaller particle sizes (x around 0.024 μm). All five curves taken at the altitude of 10 km feature a similar size distribution and a comparable total particle concentration. The absence of higher concentrations of larger particles ($x > 0.05$

μm) in the well-aged aerosol indicates a possible transport from the lower stratosphere. This kind of airmass and aerosol exchange has been described already by Cadle and Kiang (1977). The other samples in Figs. 6 and 7 feature differently shaped size distribution curves. Because several of the samplings were performed in cirrus clouds, a very interesting interpretation of the observed lower concentrations of small particles (with $x < 0.03$ μm) and particles larger than 0.10 μm can be made following the theoretical study of the scavenging rates of submicron aerosol particles by ice crystals by Miller (1990). The author neglected inertial forces for submicron aerosol and considered only Brownian diffusion, thermophoresis, diffusiophoresis, and electrostatic attraction. In the very small particle size range, Brownian diffusion dominates the deposition process on differently shaped crystals characterized by their capacitance. Phoretic forces and electrostatic charge affect the deposition of particles larger than 0.1 μm. Their deposition is supported by high relative humidity in and around clouds and by high air temperature gradients around cloud elements.

For the reasons mentioned before and for the difficult evaluation of impactor samples mentioned by several investigators (e.g., Blifford and Ringer 1969; Cadle et al. 1969), the large and coarse particle concentration measurements must be interpreted very cautiously. The application of different correction factors (e.g., for isokinetic sampling conditions for coarse particles) may affect seriously the presented data. Another important factor can be the simple evaluation of the number of particles under a specific nozzle. This investigation considers the homogeneous main deposition of particles under a specific ideal nozzle (no edge effects). No particle bouncing off is included, which in the case of gelatin-covered impactor glass slides depends on temperature and environmental humidity. Under the above-mentioned assumptions the total concentrations of particles (with $r > 0.25$ μm) on 14, 22, 26, and 30 November and 7 December 1991 are (large and coarse particle concentrations not corrected for isokinetic sampling are given in parentheses) 1.69741 (3.4147), 0.12765 (0.26396), 0.93459 (1.83251), 0.25872 (0.55453), and 0.69636 (1.4156) cm^{-3}. These values are a little higher than those reported, for example, by Blifford and Ringer (1969), but are comparable to the

data obtained by impactor sampling at cirrus level over the central parts of the United States in 1990 (Podzimek et al. 1994).

Clouds and high relative humidity have an important effect on the concentration and size distribution of large and coarse insoluble particles (e.g., see Hudson et al. 1991). Particles sampled in cirrus clouds have usually broader size distributions (Briehl 1974). To measure this correlation, the ratio of standard deviation σ (deduced from the ideal lognormal particle size distribution) to the mean particle size $\bar{r}$ was calculated for all measurements at relative humidities greater and smaller than 75%. From the 26 November and 5 and 6 December samples with RH > 75%, $\bar{\sigma}/\bar{r} = 0.6434$ was found, as was described earlier, and from 17 and 26 November and 5 and 6 December samples with RH < 75%, $\bar{\sigma}/\bar{r} = 0.2886$. This demonstrates clearly the effect relative humidity (or cloud) exerts on the particle aggregation and on the mean insoluble particle size and mean particle size distribution curve. The measurements also support the application of the lognormal size distribution function for particle radii between 0.75 μm and 2.00 μm.

The investigation of particle deliquescence gave mean values for $\bar{R}((NH_4)_2SO_4) = 0.0741$ and $\bar{R}(H_2SO_4) = 0.0514$ from 20 individual samplings, which are smaller than those calculated from several measurements in 1990 (Podzimek et al. 1994). However, there is a considerable scatter of soluble mass fraction $\bar{R}$ in Table 4. An attempt was made to correlate the soluble mass fraction for particles with the aerosol concentration or with the particle mean size. None of these correlations, possibly important for the question of how far the jet engine exhaust with freshly generated particles can affect the water phase transition, was found to be significant.

The qualitative identification of the nature of coarse particles has only a rough character because only 31 particles with typical shapes were evaluated. In comparison to a previous sampling the high content of carbon, sulfur, and aluminum was confirmed with the presence of silicon, chlorine, and calcium, which were also present in the background. Contrary to the previous finding of a large barium content (Hagen et al. 1994; Podzimek et al. 1994), the samples showed only small amounts of barium, much smaller than sodium, magnesium, phosphorus, potassium, and iron. There was a considerable heterogeneity concerning the composition of particles sampled at different altitudes and at different sampling times. One can speculate that most of the particles represent typical tropospheric aerosol (soil minerals, pollutants), several of the coarse particles may be derived from the jet engine effluents, and a few of them (compounds of sulfur, iron, aluminum, titanium, etc.) could have a stratospheric origin (see Cadle et al. 1969; Yamato and Ono 1989).

In pursuit of information relating to the possible process of ice crystal generation at high altitudes, as briefly

mentioned in the introduction, an attempt was made to find cloud droplets in the impactor samples taken at temperatures below $-38°C$. Impactor samples of aerosol and cloud element particles deposited on glass slides coated with a sensitized gelatin layer and taken at specific temperatures (altitudes) do not indicate, in general, that cloud drops can exist at very low temperature in cirrus clouds (on 21 Nov, $-54°C$; on 26 Nov, $-50°C$; on 21 Nov, $-54°C$; and on 28 Nov, $-46°C$). Only two drops out of several hundred imprints of cloud elements were found on the 7 December ($-38°C$) sample. Completely different results were found from the analysis of the 14 November sample taken at $-26.5°C$ at an altitude of 7.8 km. Approximately 90 drops were found along with 510 crystal imprints. The maximum frequency in the droplet size distribution corresponded to $r = 8.50$ μm. Seven droplet imprints were, however, identified in the 21 November sample taken at $-54°C$. The droplets were much larger (radii between 8 and 25 μm) and had a dark, probably insoluble, core. From the wrinkled edge of the Liesegang circles formed in the sensitized gelatin layer (by $BaCl_2$) around the core, one may conclude that 5.4% of the total concentration contained a considerable amount of sulfates. Chloride ions were identified in less than 2.5% of the total number of droplets.

7. Conclusions

Aerosol at cirrus cloud level was investigated by aircraft-based sampling during the FIRE program in November and December 1991. Condensation nuclei concentration and size distribution were determined by a TSI condensation nucleus counter (Model 3760) combined with an electrostatic aerosol classifier. Particle deliquescence was investigated with the aid of two classifiers in series, with a saturator in between them, and a TSI CN counter. The first classifier selected a quasi-monodisperse dry aerosol, which after being allowed to equilibrate to 100% relative humidity during passage through a water vapor saturator, was analyzed with the aid of the second classifier and the TSI CN counter. Large and coarse particles were deposited on slides coated with a sensitized gelatin layer, which were inserted into a UNICO inertial impactor. From the evaluation of measurements and samples taken during seven research flights over the central part of the United States at altitudes between 6 km and 11.9 km, the following conclusions were reached:

1) A large variability was observed in CN concentration at the same level of the upper troposphere during sampling intervals of several minutes duration. However, the calculated mean concentrations and their dependence on altitude do not deviate from data published by other investigators.

2) Close to the tropopause, aerosol layers of high particle concentration were observed on several occasions.

3) Cirrus clouds were usually characterized by a flat aerosol size distribution curve in the size range 0.03 $\mu m < x < 0.1$ μm with, however, lower particle concentrations in the domain of smaller and larger particles.

4) Two major types of CN distribution curves were found in and around cirrus clouds. One is simulated well by the lognormal distribution function, and the other is characterized by higher concentrations of very small particles and a "saddle" type of size distribution curve. It is hypothesized that the latter type of curve indicates the interaction of tropospheric and stratospheric aerosols.

5) Analysis of impactor samples indicated that it was rare to find liquid drops among the ice crystal elements at temperatures at or below $-38°C$.

6) Assuming the soluble species to be either pure $(NH_4)_2SO_4$ or H_2SO_4, deliquescence measurements and standard cloud microphysical calculation lead to the conclusion that in the investigated particle size range the corresponding soluble mass fractions are 0.0741 and 0.0514, respectively.

7) A study of large and coarse particles via impactor samplings reveals that their concentrations may be between several tenths and 1.7 cm^{-3} with a roughly lognormal size distribution curve. Their composition is dominated by the presence of sulfur, carbon, chlorine, as well as soil minerals.

REFERENCES

Alofs, D. J., 1978: Performance of a dual-range cloud nucleus counter. *J. Appl. Meteor.,* **17,** 1286–1297.

——, and M. B. Trueblood, 1981: UMR Dual Mode CCN Counter (Modes: CFD plus Haze). *J. Rech. Atmos.,* **15,** 219–223.

——, ——, D. R. White, and V. L. Behr, 1979: Nucleation experiments with monodisperse NaCl aerosols. *J. Appl. Meteor.,* **18,** 1106–1117.

——, D. E. Hagen, and M. B. Trueblood, 1989: Measured spectra of the hygroscopic fraction of the atmospheric aerosol particles. *J. Appl. Meteor.,* **28,** 126–136.

Badzioch, S., 1960: Correction for anisokinetic sampling of gasborne dust particles. *Brit. J. Inst. Fuel.,* **33,** 106–110.

Blifford, I. H., and L. D. Ringer, 1969: The size and number distribution of aerosols in the continental troposphere. *J. Atmos. Sci.,* **26,** 716–726.

Briehl, D., 1974: In situ measurement of particulate number density and size distribution from an aircraft. NASA Tech. Memo. NASA TMX-71577, 12 pp.

Cadle, R. D., and C. S. Kiang, 1977: Stratospheric Aitken particles. *Rev. Geophys. Space Phys.,* **15,** 195–202.

——, R. Bleck, J. P. Shedlovsky, I. H. Blifford, J. Rosinski, and A. L. Lazrus, 1969: Trace constituents in the vicinity of jet streams. *J. Appl. Meteor.,* **8,** 348–356.

Davies, C. N., 1968: The sampling of aerosols. *Staub-Reinhalt. Luft,* **28,** 219–225.

Fitzgerald, J. W., C. F. Rogers, and J. G. Hudson, 1980: Review of isothermal haze chamber performance. *Proc. Third Int. Cloud Condensation Nuclei Workshop,* Reno, NV, NASA, p. 85.

Frenzel, A., and F. Arnold, 1994: Sulfuric acid cluster ion formation by jet engines: Implications for sulfuric acid formation. *Impact of Emissions from Aircraft and Spacecraft upon the Atmosphere. Proc. of Int. Scientific Colloquium,* Koln, Germany, German Aerospace Research Establishment, 106–112.

Hagen, D. E., and D. J. Alofs, 1983: A Linear inversion method to obtain aerosol size distributions from measurements with a differential mobility analyzer. *Aerosol Sci. Technol.,* **2,** 465–475.

——, M. B. Trueblood, and P. D. Whitefield, 1992: A field sampling of jet exhaust aerosols. *Part. Sci. Technol.,* **10,** 53–63.

——, J. Podzimek, A. J. Heymsfield, M. B. Trueblood, and C. K. Lutrus, 1994: Potential role of heterogeneous nucleation in the cloud element formation at high altitudes. *Atmos. Res.,* **31,** 123–135.

Heymsfield, A. J., 1972: Ice crystal terminal velocities. *J. Atmos. Sci.,* **29,** 1348–1351.

——, 1973: The cirrus uncinus generating cell and the evolution of cirroform clouds. Ph.D. dissertation, University of Chicago, 269 pp.

——, 1975a: Cirrus uncinus generating cells and the evolution of cirroform clouds. Part II: The structure and circulations of the cirrus uncinus generating head. *J. Atmos. Sci.,* **32,** 809–819.

——, 1975b: Cirrus uncinus generating cells and the evolution of cirroform clouds. Part III: Numerical computations of the growth of the ice phase. *J. Atmos. Sci.,* **32,** 820–830.

——, 1977: Precipitation development in stratiform clouds: A microphysical and dynamical study. *J. Atmos. Sci.,* **34,** 367–381.

——, and C. M. R. Platt, 1984: A parameterization of the size spectrum of ice clouds in terms of the ambient temperature and ice water content. *J. Atmos. Sci.,* **41,** 846–855.

——, and R. M. Sabin, 1989: Cirrus crystal nucleation by homogeneous freezing of solution drops. *J. Atmos. Sci.,* **46,** 2252–2264.

Hudson, J. G., J. Hallett, and C. F. Rogers, 1991: Cloud formation by combustion aerosol. *J. Geophys. Res.,* **96,** 10 847–10 859.

Junge, C. E., C. W. Chagnon, and J. E. Manson, 1961: Stratospheric aerosols. *J. Meteor.,* **18,** 81–108.

Liou, K., 1986: Influence of cirrus clouds on weather and climate processes: A global perspective. *Mon. Wea. Rev.,* **114,** 1167–1199.

Miller, N. L., 1990: A model for the determination of the scavenging rates of submicron aerosols by snow crystals. *Atmos. Res.,* **25,** 317–330.

Parungo, F., 1995: Ice crystals in high clouds and contrails. *Atmos. Res. (Weickmann Memorial Volume),* in press.

Podzimek, J., 1990: Peculiarities of submicron aerosol (Aitken nuclei) distribution around the tropopause. *Proc. 83rd Annual Meeting Air and Waste Management Association,* Pittsburgh, PA, Air and Waste Management Association, 90–144.5.

——, W. A. Sedlacek, and J. B. Haberl, 1977: Aitken nuclei measurements in the lower stratosphere. *Tellus,* **29,** 116–127.

——, H. D. Ayres, and J. Mundel, 1984: Isokinetic sampling problem. *Aerosols* B. Y. H. Liu, D. Y. H. Pui, and H. Fissan, Eds., Elsevier Scientific, 159–162.

——, K. M. Issac, and B. Husen, 1991. Aerosol particle bouncing in cascade impactors. *Developments in Mechanics,* Vol. 16, R. C. Batra and B. F. Armaly, Eds., Department of Mechanical and Aerospace Engineering, University of Missouri at Rolla, 376–377.

——, D. E. Hagen, and E. Robb, 1995: Large aerosol particles in cirrus clouds. *Atmos. Res.* (Weickmann Memorial Volume) **38,** 263–282.

Pruppacher, H. R., and J. D. Klett, 1978. *Microphysics of Clouds and Precipitation.* Reidel, 714 pp.

Rader, D. J., and P. H. McMurry, 1986: The tandem differential mobility analyzer. *TSI J. Particle Instrum.,* **1,** 3–14.

Sassen, K., and G. C. Dodd, 1989: Haze particle nucleation simulations for numerical and lidar studies. *J. Atmos. Sci.,* **46,** 3005–3014.

——, D. Starr, and T. Uttal, 1989: Mesoscale and microscale of cirrus clouds: Three case studies. *J. Atmos. Sci.,* **46,** 371–396.

——, ——, G. Mace, M. Poellot, S. Melfi, W. Eberhard, J. Spinhirne, E. Eloranta, D. Hagen, and J. Hallet, 1994: The 5–6 December 1991 FIRE IFO II jet stream cirrus case study: The influence of volcanic aerosols. *J. Atmos. Sci.,* **52,** 97–123.

Starr, D. O'C., 1987: Intensive field observations planned for FIRE. *Bull. Amer. Meteor. Soc.,* **68,** 119–124.

Stephens, G. L., 1980: Radiative properties of cirrus clouds in the infrared region. *J. Atmos. Sci.,* **37,** 435–446.

——, T. S.-C. Tsay, P. W. Stackhouse Jr., and P. J. Flatau, 1990: The relevance of the microphysical and radiative properties of cirrus clouds to climate and climatic feedback. *J. Atmos. Sci.,* **47,** 1742–1753.

Watson, H. H., 1954: Errors due to anisokinetic sampling of aerosols. *Amer. Ind. Hyg. Assoc. Quart.,* **15,** 21.

Weickmann, H., 1948: *The Ice Phase in the Atmosphere.* Royal Aircraft Establishment, 95 pp.

Wilson, J. C., W. T. Lai, and S. D. Smith, 1991: Measurements of condensation nuclei above the jet stream: Evidence for cross jet transport by waves and new particle formation at high altitude. *J. Geophys. Res.,* **96,** 17 415–17 423.

Yamato, M., and A. Ono, 1989: Chemical and physical properties of stratospheric aerosol. Particles in the vicinity of tropopause folding. *J. Meteor. Soc. Japan,* **67,** 147–165.

Yue, P. C., and J. Podzimek, 1980: Potential use of chemical spot test method for submicron aerosol sizing. *Ind. Eng. Chem. Prod. Res. Dev.,* **19,** 42–46.